Introduction

An airfoil is an aerodynamic shape that is used to generate lift or downforce (in Formula 1 cars). Airfoils are also used in turbomachinery such as turbine and compressors. An airfoil has a chord and a mean camber line (if it is non-symmetric). A chord is a straight line that connects the leading and the trailing edge. Whereas the camber line is mean line drawn between the top and bottom of the airfoil. A camber line and the chord are the same for a symmetric airfoil. Symmetric airfoils are often used as stabilizing surfaces in an aircraft. Such as the aircraft horizontal tail [3].

We assume that an airfoil is moving through the air or the air moving over the airfoil at a certain angle from the chord line (angle of attack). For a cambered airfoil, even at a zero angle of attack, there will be some lift. As the air passing over the suction side of the airfoil will have to travel faster to meet the flow at the same time at the trailing edge. This acceleration of the flow will create suction due to Bernoulli's theorem. The flow at the trailing edge leaves smoothly and cannot reverse over the top or bottom surface, which is also known as the Kutta condition [4].

Another explanation of why lift is produced is due to the net circulation on the airfoil. The circulation is given by the Kutta – Joukowski theorem as $\Gamma = \rho V L'$, where L' is the lift per unit span. Therefore, according to this theorem, the higher the circulation, the higher the lift [4].

Lift coefficient also has a mostly linear relationship with the angle of attack. As the angle of attack increases, the lift increases. But there will come an angle of attack which is too high. This is where flow separation occurs, and this causes loss in lift instead. So, increasing the angle of attack beyond this point will keep the airfoil or aircraft stalled which is not a good idea[5].

Vortex panel method is a method that divides the airfoil into different panels. A control point is then fixed at the midpoint of the panel. A vortex of circulation strength Γ is then placed over this control point. The vortex strength for that panel is assumed to be constant. If we take a panel, we can observe that the vortex strengths from the other panels will increase its overall circulation. In the next sections we will describe this method into more detail.

Thin airfoil theory is a theory that suggest that we assume the airfoil to be very thin. So thin in fact that it can be assumed to be its camber line. Making this assumption, we can get approximate values which will be in a good accordance with the experimental values.

Finite wing theory now assumes that a wing is finite and has a wingspan. As there is a higher pressure at the bottom of the wing compared to the top, there will be vortices formed along the wingtip. These vortices will create an induced velocity which will change the angle of attack as well as the total lift produced. These vortices will also generate an induced drag. To solve this problem, we assume a vortex sheet in the shape of horseshoe vortices along the span aft of the wing. These vortices produce a higher circulation at the root or the midspan of the wing. The lift produced by the 3D wing will always be less than the lift produced by 2D wings with infinite span.

Methods and Calculations

Airfoil Profile Generation

Before we calculate the pressure distribution and the lift produced on the airfoil, we must generate the airfoil profile along with its camber line. For a four-digit NACA airfoil of the form NACA 1410, the

first digit '1' is used to represent the maximum camber in percentage of the chord length. The second digit '4' is used to represent the location of the maximum camber from the leading edge of the chord. Its value is $1/10^{th}$ of the chord length. And finally, the last two digits '12' are used for the maximum thickness of the airfoil in percentage of the chord. So, for our airfoil,

Maximum camber $= m = 1/100 = 0.01$

Location of maximum camber $= p = 4/10 = 0.4$

Maximum thickness $= t_{max} = 10/100 = 0.10$

The mean camber line can then be plotted using the piecewise function as follows [4]:

$$z_c = \begin{cases} \dfrac{m}{p^2}[2px - x^2] & ; 0 \le x < p \\ \dfrac{m}{(1-p)^2}[(1-2p) + 2px - x^2] & ; p \le x \le 1 \end{cases}$$

The thickness distribution for a closed trailing edge can then be shown by:

$$t_c = 5t_{max}\left[0.2969\sqrt{x} - 0.126x - 0.3516x^2 + 0.2843x^3 - 0.1036x^4\right]$$

Upper portion of the airfoil or the suction surface can be represented by:

$$x_u = x - t_c sin\theta \; ; \; z_u = z_c + t_c cos\theta$$

Similarly, the lower surface or the pressure surface is given by:

$$x_L = x + t_c sin\theta \; ; \; z_L = z_c - t_c cos\theta$$

The angle here comes from the slope of the airfoil as follows:

$$\theta = tan^{-1}\left(\frac{dz_c}{dx}\right)$$

The differential can be calculated by the different piecewise mean camber line functions which gives:

$$\frac{dz_c}{dx} = \begin{cases} \dfrac{2m}{p^2}[p - x] & ; 0 \le x < p \\ \dfrac{2m}{(1-p)^2}[p - x] & ; p \le x \le 1 \end{cases}$$

With this information we can now plot the airfoil for any NACA four-digit airfoil. We do it using the MATLAB code provided in the appendix.

For our analysis, we observe that by linearly spacing the coordinates we do not get a good approximation of the airfoil shape at the leading and the trailing edge. Therefore, we use cosine function to approximate the points. The equation is given as follows [6]:

$$x = \frac{1}{2}(1 - cos\psi) \; ; 0 \le \psi \le 2\pi$$

Where ψ is linearly spaced using the number of points. We choose the number of points equal to 40. The resulting airfoil along with the points is shown by the figure below:

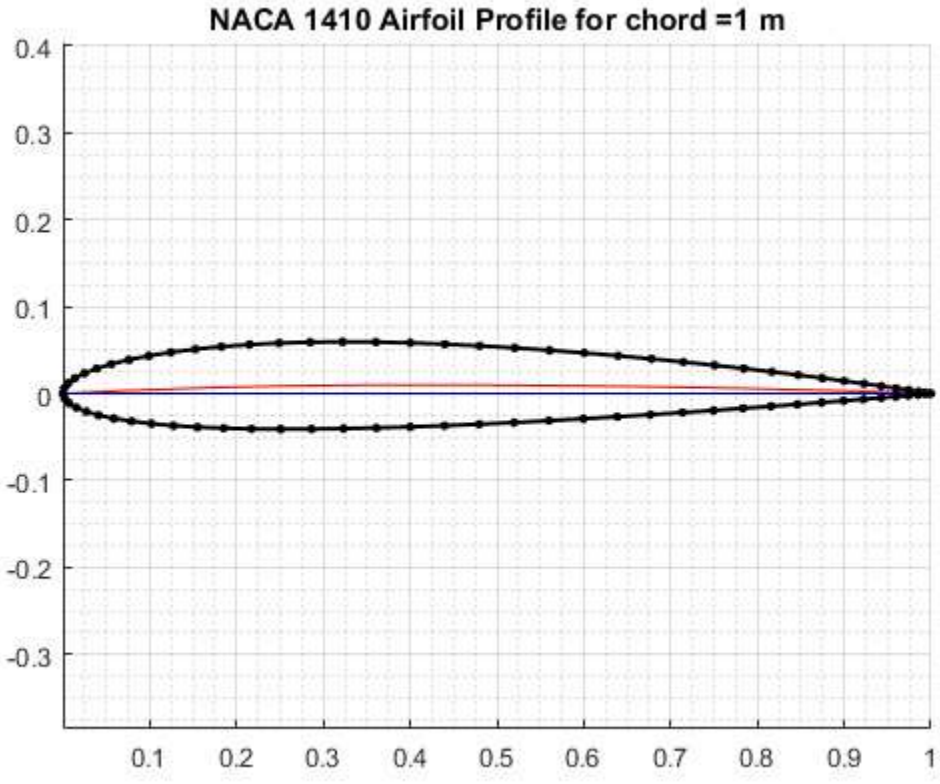

Figure 1: NACA Airfoil Profile

Vortex Panel Method

With the airfoil profile now generated, we will divide it into panels and apply vortices at the center of each panel. Also, described as the vortex panel method.

We will use the method described by Kuethe and Chow[1]. Before we begin dividing the panels, we must conjoin the two surfaces (suction and pressure) into one surface. The conjoined surface must also have its first point (j=1) at the trailing edge of the airfoil and the last point (j = m) at the trailing edge of the suction surface. We must also remove the repeating point at the leading edge for both surfaces while conjoining them into one.

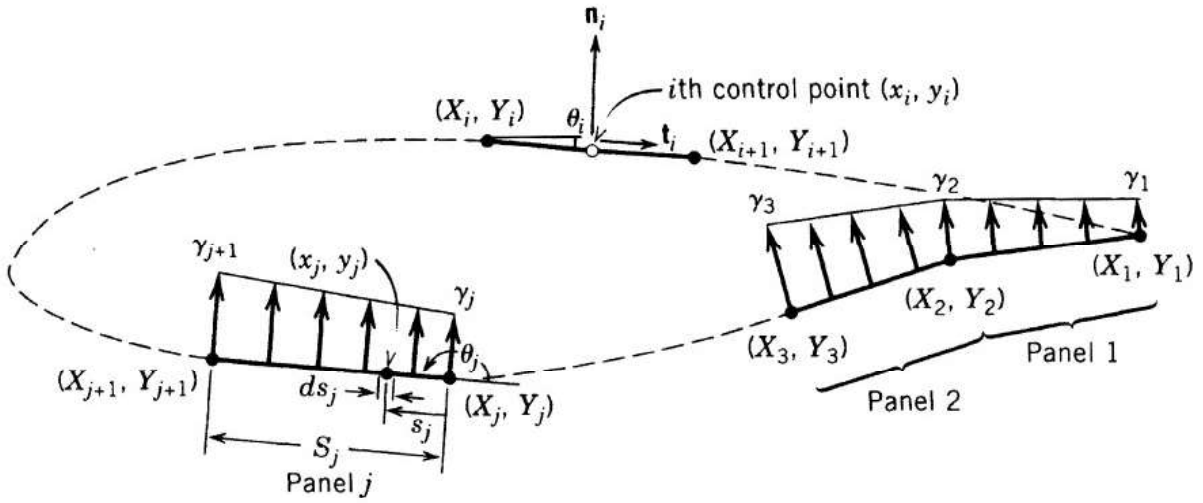

Figure 2: Vortex Panel Method [1]

As described by figure 2, the airfoil is divided into panels using the airfoil coordinates that we generated in the previous section. The panel starting and ending points are given by coordinates (X_j, Z_j) and (X_{j+1}, Z_{j+1}). The control point along is its midpoint given by (X_i, Z_i) and (X_{i+1}, Z_{i+1}). The length of the panel is denoted by S_j.

There is also a uniform flow coming from the left with a freestream velocity of V_∞ and an angle of attack of α. The total velocity potential with the uniform flow and the sum of all vortices may be written according to Kuethe and Chow as:

$$\phi(x_i, y_i) = V_\infty(x_i cos\alpha + y_i sin\alpha) - \sum_{j=1}^{m} \int \frac{\gamma(S_j)}{2\pi} tan^{-1}\left(\frac{y_i - y_j}{x_i - x_j}\right) ds_j$$

where,

$$\gamma(s_j) = \gamma_j + (\gamma_{j+1} - \gamma_j)\frac{s_j}{S_j}$$

If the surface of the airflow is considered as a streamline, there cannot be any normal velocity.

$$\frac{\partial}{\partial n_i}\phi(x_i, y_i) = 0\ ;\ \forall i$$

Numerically differentiating with respect to the normal vector, we obtain:

$$\sum_{j=1}^{m} C_{n1_{i,j}}\gamma'_j + C_{n2_{i,j}}\gamma'_{j+1} = \sin(\theta_i - \alpha)\ ;\ \forall i$$

where,

$$\gamma' = \frac{\gamma}{2\pi V_\infty}$$

$$C_{n1_{i,j}} = 0.5DF + CG - C_{n2_{i,j}}$$

$$C_{n2_{i,j}} = D + \frac{0.5QF}{S_j} - (AC + DE)G/S_j$$

$$A = -(x_i - X_j)cos\theta_j - (y_i - Y_j)sin\theta_j$$

$$B = (x_i - X_j)^2 + (y_i - Y_j)^2$$

$$C = sin(\theta_i - \theta_j)$$

$$D = cos(\theta_i - \theta_j)$$

$$E = (x_i - X_j)sin\theta_j - (y_i - Y_j)cos\theta_j$$

$$F = ln\left(1 + \frac{{S_j}^2 + 2AS_j}{B}\right)$$

$$G = tan^{-1}\left(\frac{ES_j}{B + AS_j}\right)$$

$$P = (x_i - X_j)sin(\theta_i - 2\theta_j) + (y_i - Y_j)cos(\theta_i - 2\theta_j)$$

$$Q = (x_i - X_j)cos(\theta_i - 2\theta_j) - (y_i - Y_j)sin(\theta_i - 2\theta_j)$$

Kutta condition at the Trailing Edge can be given by:

$$\gamma' + {\gamma'}_{m+1} = 0$$

Now we have m+1 equations to solve m+1 unknowns. The equation can be further simplified using influence coefficients as:

$$\sum_{j=1}^{m+1} A_{n_{i,j}}\gamma_j' = RHS\ ; i = 1,2, \ldots., m+1$$

If $i < m+1$:

$$A_{n_{i,1}} = C_{n1_{i,1}}$$

$$A_{n_{i,j}} = C_{n1_{i,j}} + C_{n2_{i,j-1}}\ ;\ j = 2,3, \ldots.m$$

$$A_{n_{i,m+1}} = C_{n2_{i,m}}$$

$$RHS_i = \sin(\theta_i - \alpha)$$

If $i = m+1$:

$$A_{n_{i,1}} = A_{n_{i,m+1}}$$

$$A_{n_{i,j}} = 0\ ;\ j = 2,3, \ldots.m$$

$$RHS_i = 0$$

We can now calculate for the circulation density as a system of linear equations. After finding the circulation densities, we now need to find the velocities to find the pressure distribution over the surface. Differentiating the potential function with respect to the tangential component and dividing by the freestream velocity, we can get the dimensionless velocity as shown:

$$V_i = \cos(\theta_i - \alpha) + \sum_{j=1}^{m} \left(C_{t1_{i,j}} \gamma'_j + C_{t2_{i,j}} \gamma'_{j+1} \right) ; \;\; i = 1,2, \dots m$$

where,

$C_{t1_{i,j}} = 0.5CF - DG - C_{t2_{i,j}}$

$C_{t2_{i,j}} = C + \frac{0.5PF}{S_j} + (AD - CE)G/S_j$

$C_{t2_{i,i}} = C_{t2_{i,i}} = \frac{\pi}{2}$

Similarly, using the influence coefficients, we can rewrite it as:

$$V_i = \cos(\theta_i - \alpha) + \sum_{j=1}^{m} \left(C_{t1_{i,j}} \gamma'_j + C_{t2_{i,j}} \gamma'_{j+1} \right) ; \;\; i = 1,2, \dots m$$

$$V_i = \cos(\theta_i - \alpha) + \sum_{j=1}^{m} A_{t_{i,j}} \gamma'_j ; \;\; i = 1,2, \dots m$$

where,

$A_{t_{i,1}} = C_{t1_{i,1}}$

$A_{t_{i,1}} = C_{t1_{i,j}} + C_{t2_{i,j-1}} ; \;\; j = 2,3, \dots . m$

$A_{t_{i,m+1}} = C_{t2_{i,m}}$

Now, Pressure Coefficient,

$$C_p = 1 - {V_i}^2$$

Lift Coefficient [4],

$$C_l = \frac{1}{c} \left[\int_0^c \left(C_{p,l} - C_{pu} \right) dx \right]$$

Moment coefficient about the Leading Edge [4],

$$C_m = -\frac{1}{c^2} \int_0^c \left(C_{p,l} - C_{pu} \right) dx$$

In the code, we do not divide by the chord length as our dx values are already non-dimensional.

C_P values for α of 0 , 8, and 16 degrees are calculated and plotted on the same curve.

Thin Airfoil Method

We can approximate the mean camber line of the airfoil using Fourier cosine series. These Fourier coefficients can then be used to find performance parameters. The first Fourier series coefficient is given by [4]:

$$A_0 = \alpha - \frac{1}{\pi}\int_0^{\pi} \frac{dz_c}{dx} d\theta$$

We calculated the differential of the mean camber line with respect to x in the previous sections. Substituting the piecewise function and

$$x = \frac{1}{2}(1 - cos\theta)$$

and

$$\eta = cos^{-1}(1 - 2p)$$

we get,

$$A_0 = \alpha - \frac{1}{\pi}(I_1 + I_2)$$

where,

$$I_1 = \int_0^{\eta} \frac{2m}{p^2}\left[p - \frac{1}{2}(1 - cos\theta)\right] d\theta$$

$$I_2 = \int_{\eta}^{\pi} \frac{2m}{(1-p)^2}\left[p - \frac{1}{2}(1 - cos\theta)\right] d\theta$$

Upon integration and simplification,

$$I_1 = \frac{m(2p\theta_h + sin\theta_h - \theta_h)}{p^2}\Bigg|_0^{\eta} \quad \text{and } I_2 = \frac{m(2p\theta_h + sin\theta_h - \theta_h)}{(1-p)^2}\Bigg|_{\eta}^{\pi}$$

For the rest of the coefficients,

$$A_n = \frac{2}{\pi}\int_0^{\pi} \frac{dz_c}{dx} \cos(n\theta) d\theta$$

We break the integrals down again and get,

$$I_3 = \frac{m[(cos\theta_h + 4p - 2)sin\theta_h + \theta_h]}{2p^2}\Bigg|_0^{\eta} \quad \text{and } I_4 = \frac{m[(cos\theta_h + 4p - 2)sin\theta_h + \theta_h]}{2(1-p)^2}\Bigg|_{\eta}^{\pi}$$

$$A_1 = \frac{2}{\pi}(I_3 + I_4)$$

$$I_5 = \frac{msin\eta[cos\theta_h(2cos\theta_h + 6p - 3) + 1]}{3p^2}\Bigg|_0^{\eta} \quad \text{and } I_6 = \frac{msin\theta_h[cos\theta_h(2cos\theta_h + 6p - 3) + 1]}{3(1-p)^2}\Bigg|_{\eta}^{\pi}$$

$$A_2 = \frac{2}{\pi}(I_5 + I_6)$$

Lift Coefficient,

$$C_l = \pi(2A_0 + A_1)$$

Moment coefficient about the Leading Edge,

$$C_m = -\frac{\pi}{2}\left(A_0 + A_1 - \frac{A_2}{2}\right)$$

C_l values for a range between 0 and 16 degrees are calculated and zero-lift angle of attack $(\alpha_{L=0}) = \alpha - C_l/(2\,\pi)$

Finite Wing Method

We have a rectangular wing with a wingspan(b) of 8m. Since the wing is rectangular,

Taper ratio = λ = 1

Root chord length = Chord length

Aspect Ratio

$$AR = \frac{2b}{c_r(1+\lambda)} = 8$$

Surface Area

$$S = {b^2}/{AR} = 8\ m^2$$

Dividing the span into 15 parts, we can get the span distribution angle (ϕ)

Chord distribution

$$c(\phi) = c_t + \left(\frac{c_r - c_t}{{\pi}/{2}}\right)\phi$$

$$\mu(\phi) = \frac{2\pi c(\phi)}{4b}$$

Now, solving the system of equations below we can find the performance characteristics of the wing [4].

$$LHS(\phi) = \sum_{i=1}^{2n-1} C_i A_i \quad ; i = 1,3,5,7, \ldots$$

where,

$LHS(\phi) = \mu(\phi)(\alpha - \alpha_{L=0})\sin(\phi)$

$C_n = (i\mu(\phi) + sin\phi)\sin(i\phi)\,; i = 1,3,5,7, \ldots$

Number of ϕ will be equal to the number of unknown coefficients. Solving this linear system of equations will give us the information we need,

Lift Coefficient,

$$C_L = \pi A_1 AR$$

Moment coefficient about the Leading Edge,

$$C_M = -C_L x_{cp}$$

We found x_{cp} in the previous section. Induced drag can be calculated by:

$$C_{D,i} = \frac{{C_L}^2}{\pi AR}(1 + \delta)$$

where,

$$\delta = \sum_{i=1}^{2n-1} i\left(\frac{A_i}{A_1}\right)^2$$

Also, plotting the non-dimensional spanwise circulation along the center or pressure. Circulation can be calculated using:

$$\Gamma(\phi) = 2bV_\infty \sum_{i=1}^{2n-1} A_i sin(i\phi)$$

For non-dimensional circulation:

$$\Gamma'(\phi) = \frac{\Gamma(\phi)}{2bV_\infty} = \sum_{i=1}^{2n-1} A_i sin(i\phi)$$

In the next section, we will compare the performance characteristics and discuss the observations made.

Results and Discussion

We ran the code provided in appendix for a NACA 1410 cambered airfoil. We tried to linearly space the points along the airfoil, but it did not generate smooth curves near the trailing edge and the leading edge. Therefore, we used a cosine series to get the airfoil coordinates as mentioned in the previous section. We calculated the lift coefficient for each case. Figure 3 below shows the variation of lift with angle of attack for three cases.

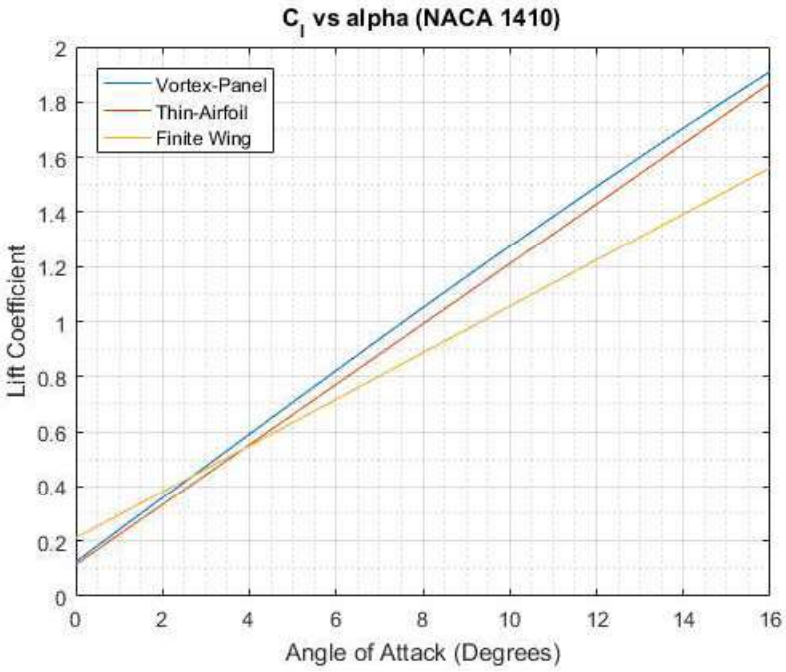

Figure 3: C_l vs Angle of Attack

As observed, the highest coefficient is given by the vortex-panel method followed by the thin-airfoil and finally the finite wing. This was expected. The vortex panel method produces the highest amount of lift because it is a 2D airfoil which has effects both from its suction side and the pressure side. Vortex panel method also does not consider any viscous or induced drag effects. The slope of the line is slightly more than 2π. The line produced through the vortex panel method is also slightly curved, it may be due to the integration error produced by the numerical trapezoidal method.

Thin airfoil theory produces a line with a slope of exactly 2π. The lift coefficient values are very close to the vortex-panel method values. Zero-lift angle of attack is higher than the vortex panel method and is also negative. This suggests that thin airfoil theory can be used for preliminary modelling of airfoils to give a close enough result with the real values.

Finally, the finite wing lift coefficient line has a smaller slope than the rest. It is because of induced drag effects caused the wingtip vortices. It also has a smaller zero-lift angle of attack. The zero-lift angle of attack using the thin airfoil method is -1.039 degrees, with the vortex panel is -1.062 degrees, with the finite wing is -2.5 degrees.

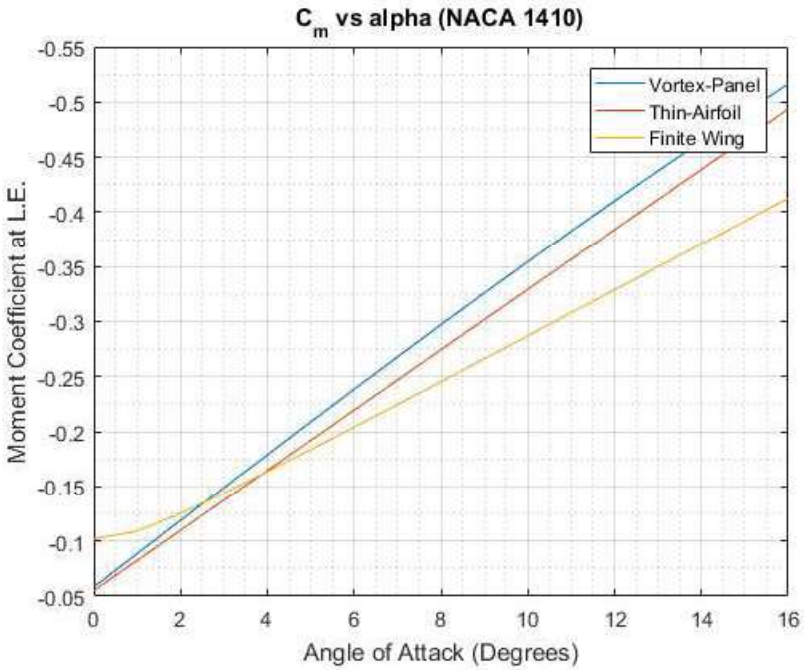

Figure 4: C_m vs Angle of Attack

When we compare the pitching moment about the Leading Edge, we find the same as before, the the moment coefficient magnitude is the highest for vortex panel method. With the lowest for the finite wing. The slopes vary with the vortex panel with the highest, then the thin airfoil, followed by the finite wing method.

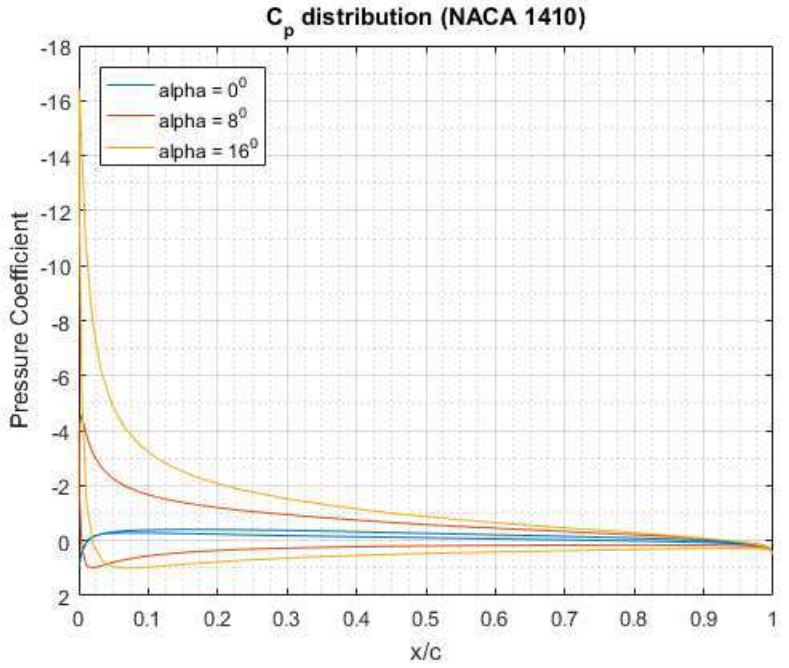

Figure 5: C_p along the chord

Cp along the non-dimensional chord length is plotted in figure 5. For zero degrees, the Cp distribution is almost zero. As the angle of attack increases, so does the pressure coefficient and the overall lifting

force. Highest magnitude of Cp always occurs at the leading edge. The suction surface has negative Cp values and the pressure surface has positive Cp values.

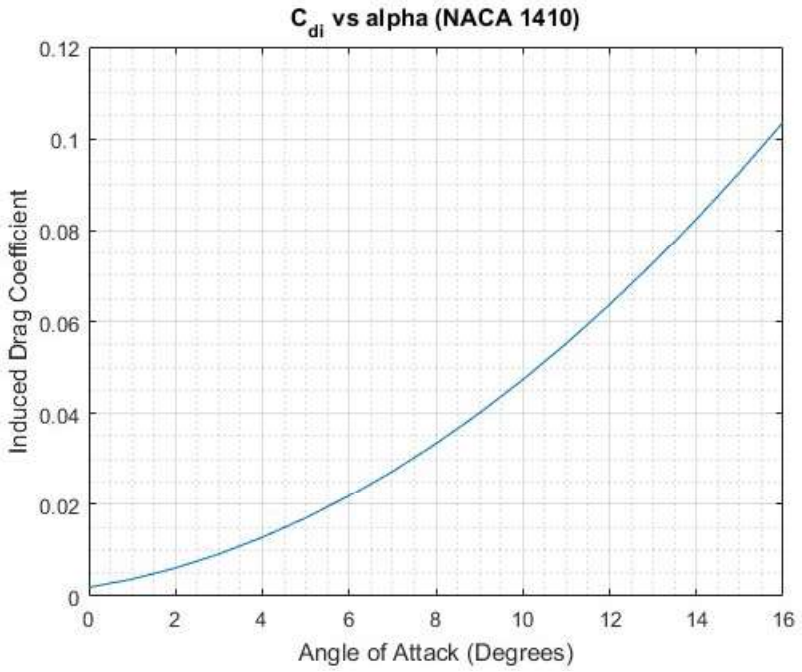

Figure 6: $C_{d,i}$ vs Angle of Attack

The induced drag produced at different angles of attack is shown by figure 6. As observed, the induced drag is the lowest at around -2.5^0 alpha and reaches a higher value as the alpha increases.

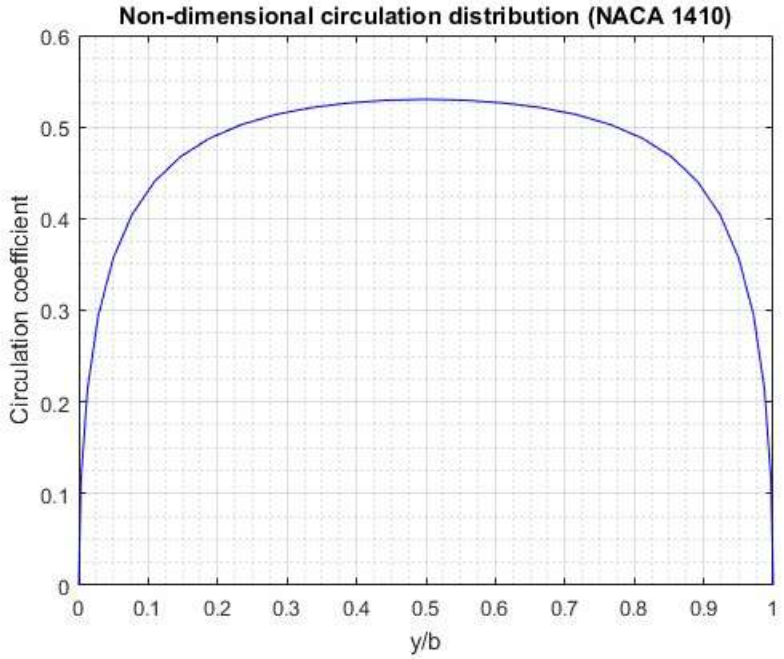

Figure 7: Circulation along the span

Figure 7 shows the circulation coefficient distribution along the non-dimensional wingspan of the finite wing taken at the center of pressure. As observed, the highest circulation happens at the middle of the wing. This implies that the peak lift or the peak lift coefficient also occurs at the mid span or where the root airfoil is.

Conclusion and Recommendations

We were able to effectively compare the data for three methods and make observations. The highest lift coefficient was produced by the vortex panel method. The highest moment at the leading edge was also produced by the vortex panel method. The zero-lift angle of attack is the lowest for the finite wing method and highest for the vortex panel method. Maximum circulation or lift occurs at the midspan or where the root airfoil is. The induced drag changes almost like an inverted parabola with the lowest induce drag happening at an angle of attack of approximately -2.5 degrees.

The code developed can be improved by adding prompts or converting it into a GUI. The users may generate and simulate any type of 4-digit NACA airfoil for the different methods. It could be used as an educational tool.

References

[1] A. M. Kuethe and C.-Y. Chow, Foundations of aerodynamics: bases of aerodynamic design. United Kingdom: J. Wiley, 2000.
[2] dpkprm, Vortex-Panel-Method, (2017), GitHub repository, https://github.com/dpkprm/Vortex-Panel-Method.git
[3] A. M. Kuethe and C.-Y. Chow, Foundations of aerodynamics: bases of aerodynamic design. United Kingdom: J. Wiley, 2000.
[4] J. Anderson, Fundamentals of Aerodynamics, 6th ed. McGraw-Hill, 2016.
[5] V. V. Sychev, “On Turbulent Boundary-Layer Separation,” Boundary-Layer Separation, pp. 91–107, 1987.
[6] jte0419, NACA_4_Digit_Airfoil, GitHub repository, https://github.com/jte0419/NACA_4_Digit_Airfoil.git